J|A|C|S ARTICLES

Published on Web 03/05/2009

Cationic and Anionic Surface Binding Sites on Nanocrystalline Zinc Oxide: Surface Influence on Photoluminescence and Photocatalysis

D. Scott Bohle* and Carla J. Spina

Department of Chemistry, McGill University, 801 Sherbrooke Street West, Montreal H3A 2K6, Quebec, Canda

Received November 4, 2008; E-mail: scott.bohle@mcgill.ca

Abstract: To probe the influence of the surface on the overall nature of zinc oxide nanocrystals (ZnO NCs) this paper examines the effects of surface modifiers: cobalt Co(II) and trimethylsilanolate, on the properties of ZnO NCs. A clear relationship between the surface, photocatalytic (PC), and photoluminescent (PL) character of ZnO is observed. With potassium trimethylsilanolate and cobalt(II) acetate we have determined that anionic binding sites occupied by silanolate contribute to 40% of the PL character of the defect emission (500−550 nm). Photodegradation of 4-nitrophenol was used as a probe to evaluate the effect of surface modification on the PC performance of ZnO NCs. At maximum silanolate modification the PC activity of ZnO was reduced by 50%. Modification of ZnO NCs with Co(II) resulted in the transfer of photoexcited electrons to the cobalt center where consequent nonradiative recombination, at energies lower than required for PC, was observed via a comparable decrease in both PL and PC activity. These results are critical for using ZnO NCs in sensory, photocatalytic, and electronic applications.

Introduction

The features of zinc oxide nanocrystals (ZnO NCs) that make them unique are also those which are not fully understood. The surface features of nanomaterials vary from the bulk and introduce new chemistry and challenges when working with inorganic materials on the nanoscale. In the photoluminescent spectrum of colloidal zinc oxide nanocrystals (NCs) two major components are observed, the ultraviolet (UV) and visible. Photoexcitation of NCs with energies greater than the band gap results in the creation of an electron−hole, exciton pair (h_{VB}^{+} + e_{CB}^{-}). The UV band gap emission results from the radiative recombination of an excited electron in the conduction band (e_{CB}^{-}) with the valence band hole (h_{VB}^{+}) and exhibits a dependence on NC size due to quantum confinement. The visible or deep trap photoluminescence (PL) is commonly defined as the recombination of the electron−hole pair from localized states with energy levels deep in the band gap, resulting in lower energy emission. These alternate energy levels are usually attributed to dopants, structural features, or surface defects.[1−8] However, the site of deep trap emission still remains controversial; there are contradictory assignments, and none explain all of the phenomena observed.[9−11] Identifying the physiochemical nature of this deep trap emission in ZnO NCs is of great importance as the UV and visible emission, as well as the photoreactivity, are all interrelated.

Many sources of the visible emission from NCs have been proposed (see Table 1). The deep trap emission was first suggested to result from a recombination event between chemisorbed $O_2^{\bullet -}$ (formed by the reduction of adsorbed O_2 by e_{CB}^{-}) on the surface and an intrinsic trapped state in the ZnO NC.[12] Later, it was proposed to be the recombination of a shallowly trapped electron with a deeply trapped hole.[2] Where the deep trap level is identified as an oxygen vacancy, $V_o^{\bullet\bullet}$ (of +2 charge in relation to O^{2-} state), $V_o^{\bullet\bullet}$ is reduced to $V_o^{\bullet}$ through the interaction of e_{CB}^{-} with a surface system O^{2-}.[2] More recent studies suggest that the surface sites facilitating visible photoluminescence are hydroxides (OH^{-}_{s}).[6] Although there has been much research on the topic, none of the current theories fully explain all of the observed phenomena associated with the luminescent qualities of ZnO NCs. In this paper we examine

(1) Van Dijken, A.; Meulenkamp, E. A.; Vanmaekelbergh, D.; Meijerink, A. *J. Phys. Chem. B* **2000**, *104*, 1715–1723.
(2) van Dijken, A.; Meulenkamp, E. A.; Vanmaekelbergh, D.; Meijerink, A. *J. Phys. Chem. B* **2000**, *104*, 4355–4360.
(3) Bahnemann, D. W.; Kormann, C.; Hoffmann, M. R. *J. Phys. Chem.* **1987**, *91*, 3789–3798.
(4) Djurisic, A. B.; Leung, Y. H. *Small* **2006**, *2*, 944–961.
(5) Lin, P.-F.; Ko, C.-Y.; Lin, W.-T.; Lee, C. T. *Mater. Lett.* **2007**, *61*, 1767–1770.
(6) van Dijken, A.; Meulenkamp, E. A.; Vanmaekelbergh, D.; Meijerink, A. *J. Lumin.* **2000**, *87−89*, 454–456.
(7) Norberg, N. S.; Gamelin, D. R. *J. Phys. Chem. B* **2005**, *109*, 20810–20816.
(8) van Dijken, A.; Meulenkamp, E. A.; Vanmaekelbergh, D.; Meijerink, A. *J. Lumin.* **2000**, *90*, 123–128.
(9) Schmidt-Mende, L.; MacManus-Driscoll, J. L. *Mater. Today (Oxford, U. K.)* **2007**, *10*, 40–48.
(10) Ozgur, U.; Alivov, Y. I.; Liu, C.; Teke, A.; Reshchikov, M. A.; Dogan, S.; Avrutin, V.; Cho, S. J.; Morkoc, H. *J. Appl. Phys.* **2005**, *98*, 041301/1−041301/103.
(11) Zhou, X.; Kuang, Q.; Jiang, Z.-Y.; Xie, Z.-X.; Xu, T.; Huang, R.-B.; Zheng, L.-S. *J. Phys. Chem. C* **2007**, *111*, 12091–12093.
(12) Lin, Y.; Wang, D.; Zhao, Q.; Li, Z.; Ma, Y.; Yang, M. *Nanotechnology* **2006**, *17*, 2110–2115.
(13) Vanheusden, K.; Warren, W. L.; Seagar, C. H.; Tallant, D. R.; Voight, J. A.; Gnade, D. E. *J. Appl. Phys.* **1996**, *79*, 7983–7990.

Table 1. Identification of Recombination Source for the Visible Emission of ZnO NCs

visible emission (eV)	proposed source[a]	refs
1.62 −2.0	$e_{CB}' + V_o$	14−16
2.1	$V_o^{\bullet} + h_{VB}^{\bullet}$	14
1.95	$V_o^{x} + V_o^{\bullet}$	2, 15, 17
2.1	$V_{Zn}'' + V_{Zn}'$	14
2.1	$Zn_i^{\bullet} + V_{Zn}'$	18−20
2.11	$OH_S' + h_{VB}^{\bullet}$	7
2.2	$e_{CB}' + V_o^{\bullet\bullet}$	1, 2, 8
2.38	$e_{CB}' + O_{Zn}$	21, 22
2.4	$V_o{:}Zn_i + h_{VB}^{\bullet}$	16
2.48	$O_2' + Tr$	3
2.61	$e_{CB}' + V_o^{\bullet}$	23
2.8	$V_{Zn}'/V_{Zn}^{x} + h_{VB}^{\bullet}$	17

[a] Kröger−Vink notation used for proposed source of visible emission in Table 1.[17] In the standard notation X_a^b, X corresponds to the species of interest, which may be an electron (e), a hole (h), a vacancy (V), or any atom. Within X_a^b, the 'a' term is the lattice site represents the lattice site occupied by species X. If the species occupies a surface site, then a = s. If the occupied site is interstitial, a = i. The 'b' term represents the value of the electric charge relative to the original site. For a null charge, b = x, for a single negative charge b = ′, and for a single positive charge, b = •.

the defect emission though surface modification studies to expand the fundamental understanding of the source of defect PL.

Modification of the NC surface has been noted to influence the PL, catalytic, and electronic properties of ZnO NCs.[7,24−28] It is crucial to understand the chemistry occurring at any nanocrystalline surface in order to control and tune the properties of the nanomaterial. To date, NC surface characterization and the correlation of structure with observed properties remain important unresolved problems. One method used to probe nanomaterial exterior involves exploring the interactions of adsorbates on the ZnO NC surface.[29−31] Organic modification, thermal passivation, or annealing the surface under a reducing atmosphere of hydrogen results in the reduction, or near elimination, of the visible fluorescence.[7] We choose to use surface modification techniques to probe the effects of adsorption on the PL and photochemistry of ZnO NCs. Through modification of the surface we are able to determine the types of surface sites that contribute to the PL and their reactivity, and to quantify these sites through PL studies and photocatalysis studies.[32,33] Potassium trimethylsilanolate, ($Me_3SiO^-K^+$), and cobalt (Co(II)) are used together to investigate electronic and surface interactions and the consequent effects on the PL spectrum and photochemical properties of ZnO NCs. In this paper we report the quenching dynamics of cobalt (Co(II)) and potassium trimethylsilanolate, the dependence of photocatalytic processes on surface modification, and the possible ZnO surface sites involved in both photoluminescence and photocatalysis. It is clear from our investigations that the surface sites of ZnO NCs must be considered inhomogeneous with both anionic and cationic sites of different coordination numbers and geometries, some of which contribute to the long disputed visible or defect emission.

Experimental Procedures

Sample Preparation. Preparation of ZnO NCs. Colloidal nanocrystalline zinc oxide (ZnO NC) is prepared at room temperature by the slow addition of tetramethylammonium hydroxide pentahydrate solution in ethanol (45 μmol, 81 μL) over 1.5 h to a rapidly stirring solution of zinc acetate dihydrate (25 μmol, 250 μL in DMSO) in DMSO (2.5 mL). Once the addition is complete, the solution is sealed and left to stir overnight to complete ripening of the nanocrystals. ZnO NC free of dioxygen modifications, are prepared by performing the reaction in an inert atmosphere box under $N_{2(g)}$ with thoroughly degassed reagents and solvents. Ultrapure ZnO NC are prepared by the same procedure, by replacing the reagent grade zinc acetate with $Zn(OAc)_2 \cdot 2H_2O$ (99.999% metal basis). For solid-state analysis nanocrystals were isolated from the DMSO solution via precipitation with ethyl acetate.

Preparation of $Me_3SiO^-K^+$-Modified ZnO NCs. Modification of the nanoparticle surface with potassium trimethylsilanolate was achieved by the post-synthesis addition of various quantities of an ethanolic solution of 0.24 M $Me_3SiO^-K^+$ to the colloidal solutions.

Preparation of Co(II)-Modified ZnO NCs. These are prepared by adding $Co(OAc)_2 \cdot 5H_2O$ (5.22 mM, in DMSO) to the freshly prepared colloidal ZnO NC solution. All samples were characterized by ultraviolet−visible (UV−vis) and photoluminescent spectroscopic techniques.

Nanocrystal Reactivity. Oxygen Reactivity. The response of ZnO NCs to oxygen was investigated utilizing the $Me_3SiO^-K^+$-modified and unmodified nanocrystals prepared under an inert nitrogen atmosphere. Ethanol (2.5 mL) and ZnO NCs (2.3 μmol, 250 μL) were combined in a Schlenk quartz cuvette under inert atmosphere. Aliquots of $O_{2(g)}$ were added to the cuvette containing the ZnO NC solution via a microsyringe. During the additions the photoluminescence of the nanocrystals was monitored spectroscopically. After each added aliquot of $O_{2(g)}$, the ZnO NC solutions were monitored until an unvarying emission spectrum was acquired. The above procedure was repeated using silanolate-modified nanocrystals to observe the effect of surface modification on dioxygen addition.

Photocatalytic Degradation. The photocatalytic activity of the silanolate-modified and unmodified ZnO NCs was examined by monitoring the photocatalytic degradation of 4-nitrophenol. Into a quartz cuvette were added ethanol (2.5 mL) and a ZnO solution (100 μL, 1 μmol, in DMSO). To the cuvette was then added 4-nitrophenol (0.17 μmol, 33.5 mM in ethanol), and the stirred solution was irradiated using a Mercury-lamp (450 W) for one

(14) Lima, S. A. M.; Sigoli, F. A.; Jafelicci, M., Jr.; Davolos, M. R. *Int. J. Inorg. Mater* **2001**, *3*, 749–754.
(15) Sukkar, M. H.; Johnson, K. H.; Tuller, H. L. *Mater. Sci. Eng., B* **1990**, *B6*, 49–59.
(16) Xu, P. S.; Sun, Y. M.; Shi, C. S.; Xu, F. Q.; Pan, H. B. *Nucl. Instrum. Methods Phys. Res., Sect. B* **2003**, *199*, 286–290.
(17) Kröger, F. A. *The Chemistry of Imperfect Crystals*, 2nd revised ed.; North-Holland Publishing Co: Amsterdam, 1973.
(18) Ramanachalam, M. S.; Rohatgi, A.; Carter, W. B.; Schaffer, J. P.; Gupta, T. K. *J. Electron. Mater.* **1995**, *24*, 413–19.
(19) Liu, M.; Kitai, A. H.; Mascher, P. *J. Lumin.* **1992**, *54*, 35–42.
(20) Riehl, N. *J. Lumin.* **1981**, *24−25*, 335–341.
(21) Lin, B.; Fu, Z.; Jia, Y. *Appl. Phys. Lett.* **2001**, *79*, 943–945.
(22) Wand, D.-F.; Liao, L.; Li, J.-C.; Fu, Q.; Peng, M.-Z.; Zhou, J.-M. *Chin. Phys. Lett.* **2005**, *22*, 2084–2087.
(23) Kamat, P. V.; Patrick, B. *J. Phys. Chem.* **1992**, *96*, 6829–6834.
(24) Yang, C. L.; Wang, J. N.; Ge, W. K.; Guo, L.; Yang, S. H.; Shen, D. Z. *J. Appl. Phys.* **2001**, *90*, 4489–4493.
(25) Chang, M.; Cao, X. L.; Zeng, H.; Zhang, L. *Chem. Phys. Lett.* **2007**, *446*, 370–373.
(26) Gong, Y.; Andelman, T.; Neumark, G. F.; O'Brien, S.; Kuskovsky, I. L. *Nanoscale Res. Lett.* **2007**, *2*, 297–302.
(27) Soares, J. W.; Whitten, J. E.; Oblas, D. W.; Steeves, D. M. *Langmuir* **2008**, *24*, 371–374.
(28) Tang, E.; Tian, B.; Zheng, E.; Fu, C.; Cheng, G. *Chem. Eng. Commun.* **2008**, *195*, 479–491.
(29) Liu, Y.; Tong, Y. *J. Nanosci. Nanotechnol.* **2008**, *8*, 1101–1109.
(30) Serpone, N.; Dondi, D.; Albini, A. *Inorg. Chim. Acta* **2007**, *360*, 794–802.
(31) Woell, C. *Prog. Surf. Sci.* **2007**, *82*, 55–120.
(32) Bowers, G. N., Jr.; McComb, R. B.; Christensen, R. G.; Schaffer, R. *Clin. Chem.* **1980**, *26*, 724–729.
(33) Zhang, W.; Xiao, X.; An, T.; Song, Z.; Fu, J.; Sheng, G.; Cui, M. *J. Chem. Technol. Biotechnol.* **2003**, *78*, 788–794.

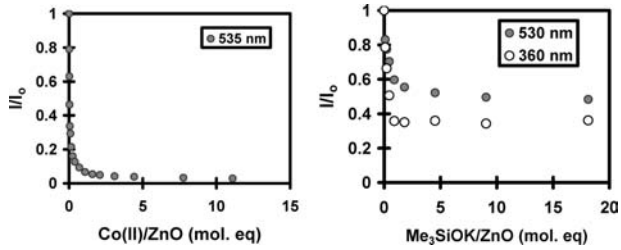

Figure 1. Effect of the addition of cobalt (Co(II)) and potassium trimethylsilanolate ($Me_3SiO^-K^+$) on the relative photoluminescent intensity of ZnO NCs $\lambda_{ex} = 342$ nm.

minute intervals followed by monitoring the photodegradation of 4-nitrophenol with UV−vis spectroscopy ($\lambda_{max} = 401$ nm). The previous photocatalytic degradation procedure was repeated using ZnO NCs modified with various concentrations of Co(II) and $Me_3SiO^-K^+$.

Physical Measurements. With the exception of the solvents employed for inert atmosphere syntheses, all chemicals and solvents were of reagent grade and used without further purification. All reagents or glassware that were to be used in the glovebox were placed under vacuum for 24 h and then transferred and stored in the inert atmosphere box for later use. Deoxygenation of solutions and solvents was performed by either distillation or freeze−pump−thaw. ZnO NC reaction solutions were used directly in further reactions with concentrations of approximately 9 μM. Absorption spectra of samples were obtained with a HP 8453 UV−visible diode array spectrophotometer. Fluorescent spectra were recorded using a FluoroMax 2 (ISA) Jobin Yvon-SPEX spectrofluorometer, with a constant excitation wavelength of 337 nm. Unless otherwise stated, the onset band-edge absorption spectra of the ZnO nanoparticles was 337 nm, and the observed emission spectra contained two peaks, a UV peak at 355 nm, and a broad visible peak at ~530 nm, the latter of which is dominant in aerated solution. Photocatalytic experiments were carried out using a Oriel Instruments Hg-lamp ($\lambda = 254$ nm) model 66033 as the excitation source.

Results

As shown in Figure 1, the addition of Co(II) to ZnO NCs results in an exponential decay of the PL intensity. Modifying the surface with trimethylsilanolate results in only 40% quenching of ZnO visible PL emission, and 65% of the UV. A red-shift in the absorption spectrum was also observed for ZnO NCs in the presence of Co(II), Supporting Information, Figure S2b, and no significant shift was observed in the absorption spectrum of silanolate-modified ZnO NCs, Supporting Information, Figure S2a. The limited quenching is interpreted as resulting from a limited number of silanolate binding sites on the ZnO surface, where the partial adsorption of silanolate results in partial quenching. As trimethylsilanolate is observed to only partially quench the ZnO visible emission, we chose to utilize the silanolate-modified ZnO (ZnO:[$^-$OSiMe$_3$], (1:1), with 40% and 65% of the visible and UV PL being quenched, respectively) system to further investigate the electronic, chemical, and physical properties of the defect states which contribute the PL of ZnO NCs.

Previous studies have established the effect of oxygen on ZnO photoluminescence, where dioxygen simultaneously promotes the visible luminescence while quenching the UV (band gap) emission[2,3,12,34] Although the exact role of oxygen in ZnO PL remains open, it is nonetheless a functional tool in the characterization, and quantization of ZnO surface structures.

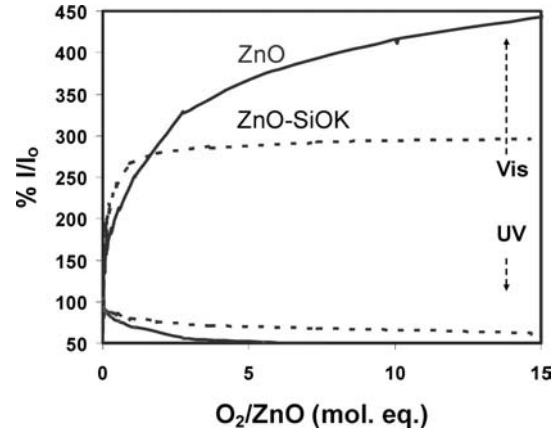

Figure 2. Effect of the addition of dioxygen to modified (with $Me_3SiO^-K^+$ - dashed) and unmodified (solid) ZnO NCs anaerobically prepared. PL trends observed above for the % relative emission intensity.

Comparison of the effect of oxygen on $Me_3SiO^-K^+$-modified and unmodified anaerobically prepared ZnO NC PL is shown in Figure 2. Silanolate modification resulted in a more rapid restoration and earlier plateau in the visible, compared to the PL of unmodified ZnO upon dioxygen addition. The plateau reached in the visible emission spectrum of silanolate-modified ZnO is attributed to the presence of adsorbed silanolate anions occupying surface sites or acting on adjacent sites which would have otherwise contributed to visible luminescence in the absence of silanolate. The inability of silanolate to interfere with all potential O_2 binding sites reinforces the presence of more than one type of surface site. Silanolate adsorption on the ZnO surface modifies and quenches one type of the surface sites, whose fluorescent contribution is approximately 40% of the total visible PL. The remaining sites have a higher efficiency for visible recombination or affinity to oxygen as they exhibit a more rapid increase of the visible emission of silanolate-modified ZnO NCs, Figure 2, dashed line. The greater affinity of oxygen to ZnO after silanolate addition is thought to be due to variation in the geometry or energetics of the defect sites adjacent to the modified sites. These stronger affinity sites contribute to the other 60% of the total visible PL. Initially the unmodified ZnO NCs require a greater quantity of oxygen for equal visible luminescent intensity, with respect to modified NCs. Addition of oxygen to unmodified NCs however, results in no discrete plateau for the visible emission at lower oxygen levels. This is indicative of the presence of a more diverse surface system with dissimilar binding affinities than those present on the modified ZnO NC surface. The chemistry of sites occupied by $Me_3SiO^-K^+$, and those remaining after modification was further investigated through analysis of the photochemical activity of the ZnO NCs.

Photoactivity of nanomaterials inherently relies on surface properties. Nanomaterials are unique in that they efficiently separate photoinduced charges, have greater solubility, and have larger surface to volume ratios, all advantageous attributes for photocatalysts.[23,35−39] Control of photocatalytic activity has previously been possible through internal and external modifica-

(34) Bohle, D. S.; Spina, C. J. *J. Am. Chem. Soc.* **2007**, *129*, 12380–12381.
(35) Bell, A. T. *Science* **2003**, *299*, 1688–1691.
(36) Dodd, A. C.; McKinley, A. J.; Saunders, M.; Tsuzuki, T. *J. Nanopart. Res.* **2006**, *8*, 43–51.
(37) Koch, U.; Fojtik, A.; Weller, H.; Henglein, A. *Chem. Phys. Lett.* **1985**, *122*, 507–510.
(38) Pearton, S. J.; Norton, D. P.; Ip, K.; Heo, Y. W.; Steiner, T. *Superlattices Microstruct.* **2003**, *34*, 3–32.

tion of nanomaterials. The inclusion of divalent metal dopants, including Ni(II), Co(II), and Mn(II), is known to decrease the photocatalytic (PC) activity of ZnO NCs.[40] The electronic activity of ZnO NCs may also be altered with surface modification as previously shown in the case of silane-modified ZnO.[27,41] The relationship between the NC surface, PL, and PC activity is exemplified in the inverse relationship between particle size and both visible PL intensity and PC activity.[8,36,40,42] This relationship between PC activity and PL and the ZnO NCs surface was elucidated by monitoring both PL and PC while varying the surface modifier concentration and identity. Quantification of the photochemical activity of ZnO NCs was accomplised via photodegradation of 4-nitrophenol (4NP), a spectrophotometric reference material.[32,33,43] Changes in the PC activity and PL with the addition of trimethylsilanolate and Co(II) were utilized to investigate the structure and character of the surface sites.

Photodegradation of 4-nitrophenol (4NP) by ZnO NCs is a known first-order PC process, Supporting Information, Figure S3, Scheme S4.[32,33,43] The PC rates of ZnO NCs, modified and unmodified, were calculated by monitoring the UV−visible absorbance ($\lambda_{max} = 401$ nm, $\varepsilon = 19200\ M^{-1}\ cm^{-1}$) of 4NP, described by eqs 1 and 2.

$$-dC/dt = k_1C \quad (1)$$

$$\ln(C_o/C_t) = k_1t \quad (2)$$

The rates of photodegradation and PL intensities were compared at variable adsorbent concentrations, Figure 3. Cobalt was found to be considerably more effective in inhibiting ZnO PC activity. The addition of 1% Co(II) results in about a 40% decrease in both PC capacity and PL. Similar trends are observed for both the PC rates and PL of ZnO NCs upon the addition of $Me_3SiO^-K^+$ with a 50% and 40% decrease in activity, respectively, after modification with one equivalent of $Me_3SiO^-K^+$. Although the PL and PC activity are interrelated, the relationship is not direct. Whether there is modification of the ZnO NC surface by trimethylsilanolate anion or Co(II), the result is a decrease in both PL and PC activity, and a clear correlation is observed. Understanding this relationship between the PL and PC activity will provide insight into the origin of the defect emission and the chemistry behind the photocatalysis which will advance our ability to utilize ZnO NCs.

Discussion

As a bulk material the ZnO wurtzite lattice is composed of three different geometric faces, two polar surfaces of opposite charge: (0001) and (000-1), and a neutral surface: (11-20), Supporting Information, Figure S5. However, the size constraints imposed by nanomaterials causes these faces to become skewed in nanoparticles and may result in a core and surface structure different from those of the bulk phase. The dependence on the PC and PL features based on size of the NCs indicates dependence on the surface to volume ratio as well as electronic confinement.[44−46] Consideration of the defects or strains in the crystal lattice due to size constraints is essential to explain the physical and chemical phenomena associated with the nanostructures. We have demonstrated that the prepared ZnO NCs have a $P6_3mc$ wurtzite hexagonal lattice from the synchrotron X-ray powder diffraction patterns, Supporting Information, Figure S8. In determining the significance and relationship of the surface with respect to the emission properties of ZnO, one must first examine the possible geometries which may be present on the nanocrystalline surface. The surface is important to consider, as interaction of adsorbates on the surface significantly influence the photochemical properties of the ZnO NCs.[26,47,48] The most common face terminations of bulk ZnO include the polar Zn-terminated (0001) and O-terminated (000-1) faces (*c*-axis oriented), and the nonpolar (11-20) faces (*a*-axis), and (10-10) faces which both contain an equal number of Zn and O atoms.[49] It is known that the faces of [0001], a polar orientation and [01-10], a nonpolar face, have anisotropic growth rates (ν): ν [0001] $\gg \nu$ [01-10] $> \nu$ [000-1]. The stability of the surfaces is also anisotropic where the polar faces have greater stability than the nonpolar faces. An inherent polarity exists in the crystal, where the character of the Zn−O bond is strongly ionic. The PC activity of the individual faces has been investigated, and the (0001) and (000-1) faces are found to be largely responsible for the majority of the PC activity of ZnO in terms of H_2O_2 production.[50] It has also been noted that defects on the (10-10) face may promote dissociative adsorption of oxygen where a spontaneous $2e^-$ charge transfer from V_o^x to O_2 ($p\pi^*$) will facilitate dissociation.[51] Oxygen dissociation results in "filling" oxygen vacancies that are present, resulting in a "healing" of the surface with an expected change in electronic properties. This type of surface alteration upon photoexcitation has been investigated by us previously.[34] Discrete facets are not the only thing to consider when dealing with ZnO NC surface structure. It is also important to account for lattice perturbations due to the inherent curvature that is not described for bulk ZnO. These lattice truncations and surface curvature must be taken into greater consideration in nanostructures even though they are rarely examined in structural detail.[9,15,31,52,53] From the observations described above it is obvious that there is more than one site contributing to the visible emission. We propose that the effects on photocatalysis and photoluminescence are due not only to electronics but also to specific surface interactions. To investigate the unique surface interactions, silanolate and cobalt

(39) Polyakov, A. Y.; Smirnov, N. B.; Govorkov, A. V.; Kozhukhova, E. A.; Pearton, S. J.; Norton, D. P.; Osinsky, A.; Dabiran, A. *J. Electron. Mater.* **2006**, *35*, 663–669.
(40) Casey, P. S.; Rossouw, C. J.; Boskovic, S.; Lawrence, K. A.; Turney, T. W. *Superlattices Microstruct.* **2005**, *39*, 97–106.
(41) Rohe, B.; Veeman, W. S.; Tausch, M. *Nanotechnology* **2006**, *17*, 277–282.
(42) Zheng, Y.; Chen, C.; Zhan, Y.; Lin, X.; Zheng, Q.; Wei, K.; Zhu, J.; Zhu, Y. *Inorg. Chem.* **2007**, *46*, 6675–6682.
(43) Marais, E.; Klein, R.; Antunes, E.; Nyokong, T. *J. Mol. Catal. A: Chem.* **2007**, *261*, 36–42.
(44) Cheng, H.-M.; Lin, K.-F.; Hsu, H.-C.; Hsieh, W.-F. *Appl. Phys. Lett.* **2006**, *88*, 261909/1–261909/3.
(45) Fu, Z. D.; Cui, Y. S.; Zhang, S. Y.; Chen, J.; Yu, D. P.; Zhang, S. L.; Niu, L.; Jiang, J. Z. *Appl. Phys. Lett.* **2007**, *90*, 263113/1–263113/3.
(46) Lin, K.-F.; Cheng, H.-M.; Hsu, H.-C.; Hsieh, W.-F. *Appl. Phys. Lett.* **2006**, *88*, 263117/1–263117/3.
(47) Hong, R.; Pan, T.; Qian, J.; Li, H. *Chem. Eng. J.* **2006**, *119*, 71–81.
(48) Wu, Y. L.; Tok, A. I. Y.; Boey, F. Y. C.; Zeng, X. T.; Zhang, X. H. *Appl. Surf. Sci.* **2007**, *253*, 5473–5479.
(49) Jagadish, C.; Pearton, S. *Zinc Oxide Bulk, Thin Films and Nanostructures: Processing, Properties and Applications*; Elsevier: Amsterdam, 2006.
(50) Jang, E. S.; Won, J.-H.; Hwang, S.-J.; Choy, J.-H. *Adv. Mater. (Weinheim, Ger.)* **2006**, *18*, 3309–3312.
(51) Ischenko, V.; Polarz, S.; Grote, D.; Stavarache, V.; Fink, K.; Driess, M. *Adv. Funct. Mater.* **2005**, *15*, 1945–1954.
(52) Shen, X.; Pederson, M. R.; Zheng, J.-C.; Davenport, J. W.; Muckerman, J. T.; Allen, P. B. *Los Alamos Natl. Lab., Prepr. Arch., Condens. Matter* **2006**, 112; http://arxiv.org/abs/cond-mat/0610002; arXiv:cond-mat/0610002 [cond-mat.mtrl-sci].
(53) Cheng, W. H.; Kung, H. H. *Surf. Sci.* **1981**, *102*, L21–L28.

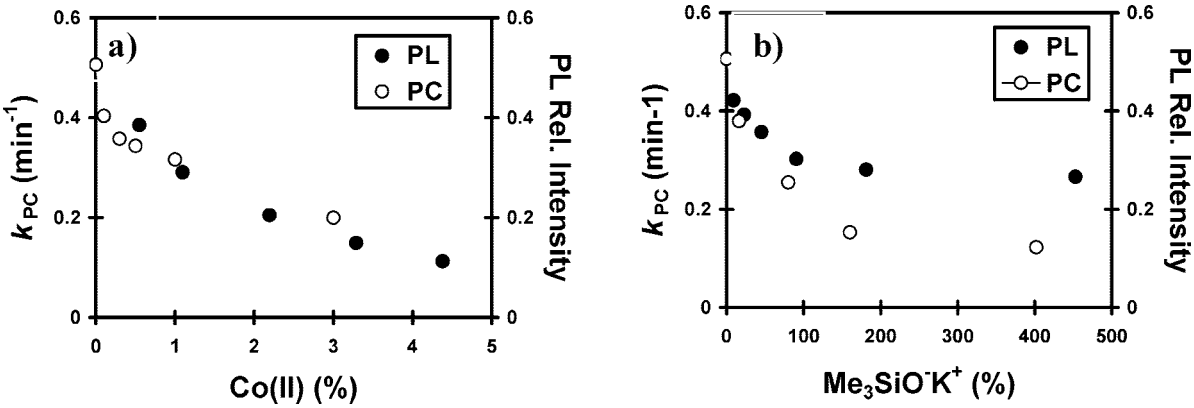

Figure 3. Comparing the photoluminescence (PL) with the rate of photocatalysis of 4-nitrophenol (PC) and with varying the percent addition, with respect to ZnO, of either (a) Co(II) or (b) $(Me)_3SiO^-K^+$.

(II) ions are used to probe the effects of cationic and anionic surface sites on the characteristics of ZnO NCs, respectively.

The origin of the green emission, $\lambda = 530$ nm, in ZnO NCs has long been debated due to its complex nature.[1−4,7,8,14,16,37] A variety of assignments for the electronic transition responsible for the broad visible emission, as shown in Table 1, involve vacancies and interstitial atoms inherently present in imperfect ZnO crystals. Other assignments involve non-innate −OH atoms present on the surface of the nanocrystal. Assigning the transitions involved in the green emission to a single-point defect is in contradiction with studies proposing donor−acceptor transitions and is an unlikely solution to the complex green emission.[54] To better understand the green emission we have utilized capping agents and dopants to manipulate the ZnO NC surface, electronic structure, and photoluminescence. In choosing the anion for surface site binding we opted for a bulky robust anion with no α or β C−H bonds. Trimethylsilanolate was chosen over *tert*-butoxide due to the relative inertness of the Si−C bonds and its lower steric bulk. Quenching the visible emission was achieved by addition of specific external or surface modifiers. In the dissociated form, anionic trimethylsilanolate caps cationic ZnO NC surface sites and quenches about half the visible emission intensity. Incomplete PL quenching indicates a limited interaction between trimethylsilanolate and the ZnO NC surface sites responsible for PL. The geometry of this binding is likened to the siloxy−ZnO aggregate structures prepared by Rell et al.[55,56] Silanolate interaction with the ZnO NC surface is proposed to be through a surface oxygen vacancy at one, two, or three Zn-coordination sites, Figure 4. Some or all of these sites are believed to be involved in the recombination, contributing to ∼40% of the visible PL. As observed by X-ray powder diffraction, Supporting Information, Figure S8, the adsorption of trimethylsilanolate on the ZnO NC surface does not alter the size or crystal structure of the nanoparticles, where only a surface interaction is inferred to be responsible for the changes in ZnO character. The involvement of these sites in PL is reinforced by the effect of silanolate-bound ZnO NCs under anaerobic conditions, where titration of oxygen into the closed system results in a more rapid, although incomplete, restoration of the visible PL, Figure 2. The change in ZnO PL response to oxygen is indicative of the presence of an absorbed species on the surface modifying O_2 adsorption and blocking potential oxygen binding sites. Changes in the PL intensity upon silanolate titration into aerobic ZnO NCs were analyzed using a Stern−Volmer plot, revealing a nonlinear trend. This result indicates that the quenching of trimethylsilanolate on ZnO NCs, Supporting Information, Figure S9, does not result from simple dynamic quenching in support of the above theory of silanolate binding on the ZnO NC surface. In an attempt to quantify the surface adsorbents we determined the Langmuir adsorption isotherms and Stern−Volmer quenching kinetics to relate the PL intensity to the fraction of occupied surface sites, as previously described by Munro et al. in the case of CdSe.[57] The PL quenching of ZnO NCs is fit to a Langmuir adsorption isotherm, Supporting Information, Figure S10.[57−61] From the Langmuir fit, assuming homogeneous adsorption, the binding constant was calculated ($K_{a,(Me)_3SiO^-} = 2500\ M^{-1}$), representing a relatively weak binding between the silanolate and ZnO NC surface. Utilizing the average ratio of ZnO and trimethylsilanolate concentrations at saturation, Supporting Information, Figure S11, we obtained an approximate value of 0.17 for the fraction of total ZnO participating in the surface interaction with trimethylsilanolate. In terms of surface fraction we consider the surface area/volume = 0.24 for ZnO NCs (radius = 2.7 nm), Supporting Information, Figure S12, where ∼70% of potential ZnO surface sites are occupied by trimethylsilanolate at saturation. Photocatalytic results may then be explained by the same adsorption effect. Trimethylsilanolate interferes with the sites and the quantity of electrons available for photocatalysis. This is observed in Figure 3b, where in the presence of various quantities of silanolate, a decreasing trend is observed for both the photodegradation rate of 4NP, and the relative intensity of the visible emission. Reduced degradation of the dye is due to occupation of surface sites by silanolate as observed by a decrease in both the rate of PC and in the visible emission, suggesting a relationship between the site responsible for the defect emission and that associated with photodegradation. The addition of an anionic surface modifier will inherently only alter cationic sites, where cationic modifying agents must be used

(54) Djurisic, A. B.; Choy, W. C. H.; Roy, V. A. L.; Leung, Y. H.; Kwong, C. Y.; Cheah, K. W.; Rao, T. K. G.; Chan, W. K.; Lui, H. F.; Surya, C. *Adv. Funct. Mater.* **2004**, *14*, 856–864.
(55) Driess, M.; Merz, K.; Rell, S. *Eur. J. Inorg. Chem.* **2000**, 2517–2522.
(56) Merz, K.; Hu, H.-M.; Rell, S.; Driess, M. *Eur. J. Inorg. Chem.* **2003**, 51–53.
(57) Munro, A. M.; Plante, I. J.-L.; Ng, M. S.; Ginger, D. S. *J. Phys. Chem. C* **2007**, *111*, 6220–6227.
(58) Kepler, K. D.; Lisensky, G. C.; Patel, M.; Sigworth, L. A.; Ellis, A. B. *J. Phys. Chem.* **1995**, *99*, 16011–16017.
(59) Lorenz, J. K.; Ellis, A. B. *J. Am. Chem. Soc.* **1998**, *120*, 10970–10975.
(60) Meeker, K.; Ellis, A. B. *J. Phys. Chem. B* **1999**, *103*, 995–1001.
(61) Zhang, J. Z.; Geselbracht, M. J.; Ellis, A. B. *J. Am. Chem. Soc.* **1993**, *115*, 7789–7793.

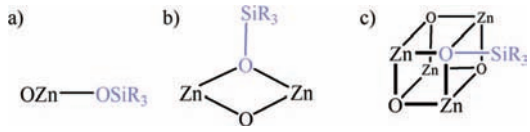

Figure 4. Potential configurations of the sites occupied by trimethylsilanolate on the surface of ZnO NCs. (a) One, (b) two, and (c) three Zn-coordinate geometries are shown.

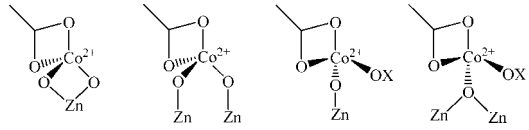

Figure 5. Possible coordination geometries for adsorbed Co (II) on the ZnO NC surface (X = H, H_2, $C(O)CH_3$).

to probe other surface sites. To accomplish this, cationic Co(II) is utilized to modify the ZnO NC surface.

Co(II) is known to act as a deep trap in II−VI semiconductors, where excitonic quenching is followed by rapid nonradiative relaxation to the ground state $^4A_2(F) \rightarrow {}^2E(G)$ (660 nm), $^4A_2(F) \rightarrow {}^4T_1(P)$ (615 nm), and $^4A_2(F) \rightarrow {}^2T_1(G)$ (568 nm).[62,63] We have shown that binding of Co(II) is reversible, as observed in its effect on ZnO NC PL, Supporting Information, Figure S6. This suggests that the same site of Co(II) binding is also involved in the ZnO PL. The geometry of the bound site is interpreted from UV−visible spectroscopy, Supporting Information, Figure S7, to be a tetrahedral environment; a transition from the octahedral geometry found in solution phase.[63] A range of possible Co(II) binding configurations on the ZnO NC surface may be hypothesized, Figure 5. The size and crystal structure of the ZnO NCs are not affected in any significant manner by the addition of Co(II), as there is no significant broadening of the Bragg peaks in the X-ray powder diffraction data, Supporting Information, Figure S8. External doping of ZnO NCs with Co(II), as shown in Figure 1, to cap anionic surface sites results in a significant loss of visible PL. The magnitude of Co(II) quenching when doped internally is enhanced, indicating a spatial barrier for electron transfer. The quenching capacity of surface-bound Co(II) is more limited. Examples of such a limited quenching radius have been observed previously in CdSe NCs.[64] The lesser quenching capacity of surface-bound Co(II) may also indicate an alternate quenching mechanism on the ZnO NC surface. The same mechanism which quenches visible PL may be responsible for the decrease in PC activity. Here the decrease in catalytic efficiency of Co(II)-doped ZnO NCs is similar to the trend for the visible emission, Figure 3a, indicative of a direct correlation between the energy levels involved in photocatalysis and the visible PL. From our data it is clear that the anionic and cationic surface sites are unique. To understand the individual influence of these sites on the overall character of ZnO NCs we need to consider the basic electronic and structural components of ZnO. In this discussion we look at the changes induced by the modifiers on the surface of the ZnO NCs. Silanolate capping of ZnO NCs results in limited suppression of the PL and PC activity of ZnO NCs. The incomplete inhibition of the PL and PC character of ZnO indicates that the sites of silanolate interaction are only a partial contributor of the PL and PC character of ZnO NCs. The possible geometries of the site or sites of silanolate binding are shown in Figure 4. The coordination of silanolate to the surface of ZnO has also been noted to alter the binding affinity of oxygen to the surface of ZnO, attributed to chemical or electronic changes of the defect sites adjacent to the silanolate-bound sites. The action of silanolate coordination through zinc results in the elimination of oxygen vacancies that were once present on the ZnO surface at those sites. The outcome of silanolate occupation of these oxygen vacancies is a finite decrease in ZnO PL. The contribution of the oxygen vacancy sites now occupied by silanolate is assigned to be the origin of the decrease observed in the visible radiative recombination. Crystal lattice faces that have the geometry required for silanolate binding are the Zn-capped (0001), (11-20) (*a*-axis), and (10-10) faces. We have successfully shown that the contributions of ZnO defects toward the visible emission are not due to a sole defect and their identification may be elucidated through specific modification of the surface. The contribution of the silanolate-occupied sites toward the visible PL was calculated to be ∼40% with ∼70% of possible surface sites on the ZnO NC occupied by trimethylsilanolate anions. Clearly all of the visible emission is not due to surface defects. The quenching of the visible emission by Co(II) also occurs through electron transfer mechanisms; additionally, a residual emission in the visible emission with surface alteration is always observed.

In previous studies ZnO photocatalytic activity was suggested to originate on the Zn-free (000-1) face and (01-10) face of the crystal. Initial reactions that occur on the ZnO NC surface are summarized by equations 3, 4, and 5.[34,50,65−69]

$$ZnO + h\nu \rightarrow ZnO(h^+_{VB} + e^-_{CB}) \quad (3)$$

$$Zn_s - O_{2abs} + e^-_{CB} \rightarrow Zn_s - O^{\bullet -}_{2abs} \quad (4)$$

$$Zn_s - O^{\bullet -}_{2abs} + e^-_{CB} + 2H^+_{aq} \rightarrow Zn_s + H_2O_2 \quad (5)$$

$$OH^-_s + h^+_{VB} \rightarrow OH^{\bullet}_s \quad (6)$$

Excitation of ZnO NCs, with an energy below the band gap, results in the separation of an exciton pair ($h_{VB}{}^+ + e_{CB}{}^-$) eq 3. When adsorbed oxygen is present on the ZnO NC, reduction of the adsorbed species may occur, eqs 4 and 5, resulting in the production of superoxide and peroxides. Surface hydroxyl and holes have also been cited as being responsible for photooxidation reactions, and in photoluminescence, where surface OH^- may undergo oxidation to form a hydroxyl radical, eq 6. [7,70−74] The proposed role of adsorbed bound oxygen (O_{2abs})

(62) Hays, J.; Reddy, K. M.; Graces, N. Y.; Engelhard, M. H.; Shutthanandan, V.; Luo, M.; Xu, C.; Giles, N. C.; Wang, C.; Thevuthasan, S.; Punnoose, A. *J. Phys.: Condens. Matter* **2007**, *19*, 266203/1–266203/24.
(63) Schwartz, D. A.; Norberg, N. S.; Nguyen, Q. P.; Parker, J. M.; Gamelin, D. R. *J. Am. Chem. Soc.* **2003**, *125*, 13205–13218.
(64) Laferriere, M.; Galian, R. E.; Maurel, V.; Scaiano, J. C. *Chem. Commun. (Cambridge, U.K.)* **2006**, 257–259.
(65) Hoffman, A. J.; Carraway, E. R.; Hoffmann, M. R. *Environ. Sci. Technol.* **1994**, *28*, 776–785.
(66) Kurtz, M.; Strunk, J.; Hinrichsen, O.; Muhler, M.; Fink, K.; Meyer, B.; Woell, C. *Angew. Chem., Int. Ed.* **2005**, *44*, 2790–2794.
(67) Polarz, S.; Strunk, J.; Ischenko, V.; van den Berg Maurits, W. E.; Hinrichsen, O.; Muhler, M.; Driess, M. *Angew. Chem., Int. Ed.* **2006**, *45*, 2965–2969.
(68) Bahnemann, D. W.; Hoffmann, M. R.; Hong, A. P.; Kormann, C. *ACS Symp. Ser.* **1987**, *349*, 120–132.
(69) Jing, L.; Yuan, F.; Hou, H.; Xin, B.; Cai, W.; Fu, H. *Sci. China, Ser. B* **2005**, *48*, 25–30.
(70) Richard, C.; Boule, P. *New J. Chem.* **1994**, *18*, 547–552.
(71) Richard, C.; Boule, P. *Sol. Energy Mater. Sol. Cells* **1995**, *38*, 431–440.
(72) Sato, S.; Kadowaki, T. *J. Catal.* **1987**, *106*, 295–300.

in the PC process of ZnO NCs, supports the involvement of a surface-bound oxygen vacancy in ZnO NC PL and PC activity.[3,68,69] The parallel observations for PL and PC activity of ZnO NCs with bound silanolate moieties may not be solely explained by the elimination of oxygen vacancies (V_o) on a Zn-free crystal face. It has been determined through oxygen addition to anaerobically prepared ZnO NCs that a combination of sites contributes to the total visible PL.[34] Occupation of surface V_o by trimethylsilanolate results in the loss of a site of visible recombination and also loss in the catalytic activity associated with that site. A relationship between PL and PC activity has previously been observed. In the comparison of nanobelts, rods, and films of ZnO it has been shown that trends in UV:visible emission intensities are comparable to the PC activity in the order belt > rod > film.[75] Anion binding or oxygen vacancies present on the ZnO NC surface appear to be pivotal for a fraction of both the PL and PC activity, both of which are affected to some degree by the adsorption of silanolate on the NC surface.

Investigations of ZnO NCs chemistry (specifically at the NC/solution interface) and the role of surface structures in the chemical and PL properties of ZnO will provide enough evidence to create a new theory to better explain the physiochemical nature of ZnO NCs. Determination of the chemical characteristics responsible for the photophysical properties and electronic structure of ZnO NCs is a fundamental step toward optimizing these nanomaterials for use in photocatalytic, sensory, and electrochemical applications. Diameter, band gap energy, redox potential, photocatalysis, and photoluminescence are interrelated properties of nanocrystals.[76] The shape, size, and exposed surface planes of semiconductor nanocrystals all play a part in the PC and PL nature of ZnO NCs. Few reports are available on the relationship between the PL and PC of ZnO NCs. In those investigations the visible emission, surface area, or defect sites have been implicated as a measure of the photocatalytic activity of ZnO NCs,[42,76−78] although in current literature, there is no consensus as to the origins and therefore the relationship between PL and PC character. Photoexcitation of ZnO NCs with energies greater than the band gap results in the creation of an exciton pair. A variety of pathways are then available to this exciton as shown in Figure 6; nonradiative decay (to either ground state or a trap state) and radiative recombination produce UV emission or visible emission, and nonradiative electron or hole transfer to species near or on the NC surface. It is the sum of these interrelated pathways that we have observed, culminating in the overall PL and PC characteristics of ZnO NCs. The PL_{UV} emission results from the direct recombination of the electron and hole, but this is a minor emission under ambient conditions. It is understood that in ZnO NCs there is an enhanced separation of charge carriers, often observed as an increase in PL_{VIS} and photocatalytic activity.[75,76] The lower energy surface defects promote the separation of charge carriers, or the transfer of electrons from the conduction band to a sub-band responsible for visible emission. The increased lifetime of the charge carriers is advantageous for photochemical reactions as it enhances the efficiency of interfacial charge transfer. The proposed origin of the sub-band, the surface defects, must then be present for visible recombination to occur. When the sites are occupied by adsorbates, this mechanism of recombination is no longer available, and a decrease in the visible emission is observed. The static quenching of silanolate indicates that there is a specific interaction of the adsorbent with the surface which is responsible for the decrease in the visible emission. The similar decrease observed in the rate of photocatalysis upon surface modification supports the involvement of these same surface defect sites in the PC process. Excitation of surface-modified ZnO NCs results in the redirection of the electrons and holes which previously were involved in PC and PL activity. Nonradiative recombination processes are then identified to account for the lost electron recombination pathways as no increase in the UV emission is observed for either silanolate or Co(II) modification (Figure 6 b). It is clear from our results that there is a relationship between the PC, PL, and the surface of ZnO NCs. Adsorption of Co(II) and trimethylsilanolate on ZnO NCs result in changes in the PL and PC activity, indicative of both anionic and cationic features on the ZnO surface playing roles in the complicated surface photochemistry.

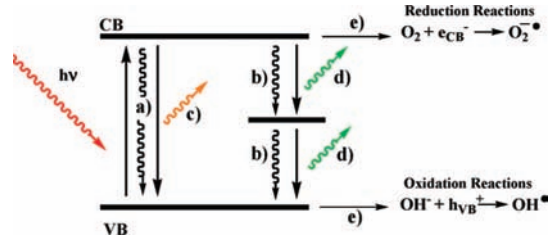

Figure 6. Photochemical pathways available to the exciton pair after photoexcitation ($h\nu$) of ZnO NCs. (a) Nonradiative recombination to ground state, (b) nonradiative recombination to a trap state or trap state to ground state, (c) radiative UV or band gap recombination, (d) radiative trap state recombination, (e) nonradiative redox reactions.

Conclusions

There are many current theories about the source of ZnO visible fluorescence. However, none of the previous theories explains all of the phenomena observed. As materials approach the nanoregime, it is well-known that the characteristics can change and that many of these changes are due to quantum confinement. However, another feature of nanomaterials is their large surface to volume ratio. It is not surprising then that physiochemical properties of ZnO NCs rely heavily on the surface which plays a large role in the changes observed as materials are scaled down to the nanoregime. The source of the controversial visible or defect emission has been theorized to originate from localized states in ZnO NCs. These states may either be found in the bulk or at the surface of a semiconductor. Defect emissions are strongly influenced by the chemical nature of the defect site and the surrounding environment. Our previous research indicated a strong influence of the surface features on the visible emission. Although the precise determination of the source of the visible emission of ZnO NCs is an ongoing process, exploitation of carefully chosen surface modifiers has brought us closer to a complete picture of the emission profile of ZnO NCs. Then with adsorbates of different charge and geometry we are able to observe the relationship between anionic and cationic sites on the nanoparticle surface and the visible emisson. By isolating these sites we have also observed

(73) Darwent, J. R.; Lepre, A. *J. Chem. Soc., Faraday Trans. 2* **1986**, *82*, 1457–1468.
(74) Dodd, A.; McKinley, A.; Saunders, M.; Tsuzuki, T. *Nanotechnology* **2006**, *17*, 692–698.
(75) Sun, T.; Qiu, J.; Liang, C. *J. Phys. Chem. C* **2008**, *112*, 715–721.
(76) Ye, C.; Bando, Y.; Shen, G.; Golberg, D. *J. Phys. Chem. B* **2006**, *110*, 15146–15151.
(77) Jing, L.; Qu, Y.; Wang, B.; Li, S.; Jiang, B.; Yang, L.; Wei, F.; Fu, H.; Sun, J. *Sol. Energy Mater. Sol. Cells* **2006**, *90*, 1773–1787.
(78) Xu, F.; Yuan, Z.-Y.; Du, G.-H.; Ren, T.-Z.; Bouvy, C.; Halasa, M.; Su, B.-L. *Nanotechnology* **2006**, *17*, 588–594.

the same effects on PC activity of ZnO NCs. The surface is fundamental to consider, as interaction of adsorbates on the surface significantly influences both the PL and photochemical properties of the ZnO NCs. This interaction may be utilized to bring us closer to understanding the true nature of the visible emission. We observed that trimethylsilanolate binding, with the possible coordination geometries mentioned above, may block anion binding surface sites which are responsible for 40% of the visible emission and 50% of PC activity. Although not all of the surface anion sites are blocked by silanolate, the modification of the surface also increases the binding affinity of oxygen to the surface. There are cation binding sites on the surface where Co(II) dynamically quenches and where electron transfer may occur, reducing both the PL and PC activity of ZnO NCs. Further study is planned for investigation into these sites with specific interest into the quenching effects of Co(II) on ZnO NCs. The sites identified may be correlated to specific faces of wurtzite ZnO structure; however, in the nanoregime, consideration of unconventional surface sites due to curvature must be considered. Current theories are less than adequate to explain all of the observed phenomena; however, with the data from previous oxygen titration experiments, the aformentioned reactions, and future experimentation, we hope to attain a more complete understanding of the surface sites and their relation to catalytic activity and photoluminescence of ZnO NCs.

Acknowledgment. We acknowledge the NSERC and CRC for generous support of this research in the form of discovery and a Canadian Research Chair for D.S.B., and to the CIHR for Chemical Biology Fellowship for C.J.S.

Supporting Information Available: Spectroscopic data including absorption, photoluminescent, and transmission electron microscopy; photocatalytic degradation detail for the decomposition of nitrophenol and the calculations of the rates of photocatalysis; analysis of the quenching dynamics and binding constants for the cationic and anionc sites on the ZnO NC surface; quantitative binding site calculations; surface area vs band gap energy relationships. This material is available free of charge via the Internet at http://pubs.acs.org.

JA808663B